Twist1 in Infiltrating Macrophages Attenuates Kidney Fibrosis *via* Matrix Metallopeptidase 13–Mediated Matrix Degradation

Jiafa Ren,[1,2] Jiandong Zhang,[1,2] Nathan P. Rudemiller,[1,2] Robert Griffiths,[1,2] Yi Wen,[1,2] Xiaohan Lu,[1,2] Jamie R. Privratsky,[3] Michael D. Gunn,[2,4] and Steven D. Crowley[1,2]

Divisions of [1]Nephrology and [4]Cardiology, Departments of [2]Medicine and [3]Anesthesiology, Durham VA and Duke University Medical Centers, Durham, North Carolina

ABSTRACT

Background Following an acute insult, macrophages regulate renal fibrogenesis through the release of various factors that either encourage the synthesis of extracellular matrix synthesis or the degradation of matrix *via* endocytosis, proteolysis, or both. However, the roles of infiltrating versus resident myeloid cells in these opposing processes require elucidation. The transcription factor Twist1 controls diverse essential cellular functions through induction of several downstream targets, including matrix metalloproteinases (MMPs). In macrophages, Twist1 can influence patterns of cytokine generation, but the role of macrophage Twist1 in renal fibrogenesis remains undefined.

Methods To study Twist1 functions in different macrophage subsets during kidney scar formation, we used two conditional mutant mouse models in which *Twist1* was selectively ablated either in infiltrating, inflammatory macrophages or in resident tissue macrophages. We assessed fibrosis-related parameters, matrix metallopeptidase 13 (MMP13, or collagen 3, which catalyzes collagen degradation), inflammatory cytokines, and other factors in these Twist1-deficient mice compared with wild-type controls after subjecting the animals to unilateral ureteral obstruction. We also treated wild-type and Twist1-deficient mice with an MMP13 inhibitor after unilateral ureteral obstruction.

Results Twist1 in infiltrating inflammatory macrophages but not in resident macrophages limited kidney fibrosis after ureteral obstruction by driving extracellular matrix degradation. Moreover, deletion of Twist1 in infiltrating macrophages attenuated the expression of MMP13 in $CD11b^{+}Ly6C^{lo}$ myeloid cells. Inhibition of MMP13 abrogated the protection from renal fibrosis afforded by macrophage Twist1.

Conclusions Twist1 in infiltrating myeloid cells mitigates interstitial matrix accumulation in the injured kidney by promoting MMP13 production, which drives extracellular matrix degradation. These data highlight the complex cell-specific actions of Twist1 in the pathogenesis of kidney fibrosis.

JASN 30: ●●●–●●●, 2019. doi: https://doi.org/10.1681/ASN.2018121253

Kidney fibrosis is a final common pathway of CKD, regardless of etiology.[1,2] The course of renal fibrogenesis includes several phases: priming, activation, execution, and progression.[3] Both hematopoietic cells and intrinsic renal cells regulate the accumulation of extracellular matrix (ECM) in the kidney, and the dynamic balance between matrix production and degradation is the ultimate determinant of kidney fibrosis progression. In response to tissue insults, heterogenous monocyte/macrophage

Received December 20, 2018. Accepted May 18, 2019.

Published online ahead of print. Publication date available at www.jasn.org.

Correspondence: Dr. Steven D. Crowley, Division of Nephrology, Department of Medicine, Durham VA and Duke University Medical Centers, DUMC Box 103015, Durham, NC 27710. Email: steven.d.crowley@duke.edu

Copyright © 2019 by the American Society of Nephrology

populations (which may be differentiated into two subsets according to their origins: Ly6C$^+$ inflammatory macrophages derived from the circulation[4] and CX3CR1$^+$ tissue-resident macrophages[5]) are activated and significantly participate in renal scar formation through (*1*) generation of proinflammatory cytokines and profibrotic factors that promote matrix deposition, or (*2*) production of enzymatic proteins to dissolve matrix and restore the renal parenchymal architecture.[6,7]

Twist1, a basic helix-loop-helix protein 38 (bHLHa38) transcription factor, regulates many biologic processes associated with fibrogenesis in the kidney. Twist1 in tubular epithelial cells engages an epithelial mesenchymal transition (EMT) program implicated in various fibrotic kidney diseases.[8] Nevertheless, scrutiny of the pericyte's role in fibrogenesis raises questions about the dominance of EMT in fibrosis,[1,9,10] and Twist1 could also attenuate ECM accumulation *via* several mechanisms. For example, Twist1 could facilitate matrix degradation by regulating the expression of several matrix metalloproteinases (MMPs).[11,12] Moreover, in immune cells, Twist1 can suppress the elaboration of inflammatory cytokines like TNF-α and IL-1β that are key players in renal fibrogenesis.[13–15] Thus, Twist1 in different cell lineages underpins biologic functions that may have discrepant effects on ECM accumulation in the kidney. To precisely manipulate the Twist1 signaling pathway in patients with renal fibrosis, a comprehensive understanding of the cell-specific contributions of Twist1 to this pathology is paramount.

We therefore sought to determine the capacity of Twist1 in macrophages to regulate the progression of kidney fibrosis, using two conditional mutant strategies to delete Twist1 selectively from either infiltrating, inflammatory macrophages or CX3CR1$^+$ tissue-resident macrophages in mice. Because we have found that the profibrotic hormone angiotensin II induces Twist1 in macrophages (data unpublished), we used the unilateral ureteral obstruction (UUO) model of activating the renin angiotensin system for our fibrosis experiments. We find that Twist1 in inflammatory macrophages derived from the circulation, but not in resident macrophages, promotes matrix metallopeptidase 13 (MMP13) within myeloid cells, enhancing matrix degradation, and attenuating renal interstitial fibrosis after UUO.

Significance Statement

Studies have shown profibrotic actions of the transcription factor Twist1 in intrinsic renal parenchymal cells. However, Twist1 expressed by immune cells can suppress inflammatory responses, and the role of macrophage-expressed Twist1 in kidney fibrosis has not been described. To study this, the authors used two conditional knockout mouse models in which *Twist1* was specifically deleted from either infiltrating or resident myeloid cells. They found that Twist1 in infiltrating myeloid cells significantly induced matrix metallopeptidase 13 (collagenase 3) generation in CD11b$^+$Ly6C^{lo} macrophages, resulting in extracellular matrix degradation and attenuation of experimental kidney fibrosis. These findings elucidate paradoxical actions of myeloid Twist1 in renal fibrogenesis, which may help facilitate design of pharmacological interventions to precisely target Twist1 while limiting off-target side effects.

METHODS

Animals

In this study, C57BL/6 floxed Twist1 mice (kind gift from Richard Behringer)[16] were crossed with C57BL/6 LysM-Cre mice to generate MKO (LysM-Cre; Twist1$^{fl/fl}$) and wild-type (WT) Cre-Twist1$^{fl/fl}$ littermates. 129/SvEv floxed Twist1 mice were crossed with 129/SvEv CX3CR1-Cre mice to generate RKO (CX3CR1-Cre; Twist1$^{fl/fl}$) mice and WT Cre-Twist1$^{fl/fl}$ littermates. Genotyping was performed to detect the presence of both flox and Cre as previously described.[17] We mapped the distributional pattern of CX3CR1-Cre recombinase expression in the UUO model by crossing with mT/mG reporter mice as we have done previously.[17] Mice were bred and maintained in the Association for Assessment and Accreditation of Laboratory Animal Care–accredited animal facilities at the Durham Veterans Affairs Medical Center according to National Institutes of Health (NIH) guidelines. All of the animal studies were approved by the Durham Veterans Affairs Medical Center Institutional Animal Care and Use Committee and conducted in accordance with the NIH Guide for the Care and Use of Laboratory Animals. Animals had free access to standard rodent chow and water. Male mice between 8 and 12 weeks old and littermate controls were used for experiments.

UUO Model of Kidney Fibrosis

UUO was performed as previously described.[17] In brief, mice were anesthetized with isoflurane, and the left ureter was isolated and ligated 3–5 mm below its origin. At 14 days after ligation, mice were euthanized and the obstructed and contralateral nonobstructed kidneys were harvested for analysis.

MMP13 Inhibitor Treatment Experiments

MKO and WT mice received MMP13 inhibitor (CL82198) at a dose of 10 mg/kg per day *via* intraperitoneal (i.p.) injection from the day of UUO to 13 days after UUO.[18,19] Mice were euthanized 14 days after UUO, and the obstructed and nonobstructed kidneys were harvested for further analysis.

Immunohistochemistry Staining for Type 1 Collagen and α-smooth muscle actin

Mouse kidney samples were fixed in 10% formalin (Sigma-Aldrich) overnight and embedded in paraffin. We used 5-μm thick sections for immunohistochemistry. To visualize interstitial collagen deposition, sections were stained with anti–type 1 collagen and α-smooth muscle actin (α-SMA). To evaluate the number of α-SMA–producing myofibroblasts, slides were stained with an antibody to α-SMA (catalog 5694; Abcam) at a 1:400 dilution as previously described.[17] On each section, eight to ten randomly selected 200× fields were then digitally photographed and scored in a blinded fashion *via* computerized morphometric analysis. Areas of positive signal were quantified by using a computer-assisted color

image analysis system (ImageJ 1.38 for Windows). Scores were averaged for each animal, and then for each group.

Hydroxyproline Assay

Kidney tissues (approximately 30 mg) were homogenized in distilled water, hydroxyproline was detected by Hydroxyproline Assay Kit (catalog ab222941; Abcam) according to the manufacturer's instructions. The hydroxyproline content was expressed as micrograms per 10 mg of kidney weight.

Western Blots

Kidney tissues (20 mg) were homogenized in RIPA buffer (Sigmal-Aldrich). Concentration of protein was quantitated using the DC Protein Assay Kit (Bio-Rad laboratories). Equal amounts of sample were subjected to electrophoresis through 4%–12% Bis-Tris Gels and transferred to polyvinylidene difluoride membranes. After blocking with 5% milk in Tris-buffered saline/Tween 20, the blots were incubated with anti–collagen type 1 antibody (catalog 1310-01; SouthernBiotech), anti–α-SMA antibody (catalog A5228; Sigma-Aldrich), anti–collagen type 4 (cat: 1340-01; Southern Biotech), anti-fibronectin (catalog 2413; Abcam), MMP13 (catalog 39012; Abcam), or anti-rabbit glyceraldehyde-3-phosphate dehydrogenase (GAPDH) (catalog 2118; CST) overnight at 4°C. The blots were then washed and incubated for 1 hour at room temperature with individual secondary antibodies accordingly. Bands were detected using an enhanced chemiluminescence detection system. The detected bands were quantified by densitometry through ImageJ 1.38 for Windows.

Collagen-Zymographic Analysis

Collagen-zymographic analysis of the MMP13 proteolytic activity in the culture media from peritoneal macrophages was performed according to a published protocol.[20] Cell culture media were collected and centrifuged at 13,000 $\times$ g for 5 minutes to remove cell debris. Centrifugal Filter Units (catalog UFC803008; Millipore) were used to concentrate proteins in the culture media. Protein was extracted from cell media, and samples were loaded into 10% SDS-polyacrylamide gel containing 0.3 mg/ml collagen (catalog C8919; Sigma-Aldrich).[20] After electrophoresis, SDS was removed from the gel by incubation in renaturing buffer (catalog LC2670; Thermo) at room temperature for 30 minutes with gentle agitation. The renaturing buffer was replaced by developing buffer (catalog LC2671; Thermo) to remove detergent with gentle agitation for 30 minutes at room temperature. The gel was then incubated at 37°C in developing buffer for 48–72 hours. Afterward, the gel was stained with a solution of 30% methanol, 10% glacial acetic acid, and 0.5% Coomassie blue R250 (catalog 27816; Sigma-Aldrich), followed by destaining in the same solution without dye. Proteinase activity was detected as unstained bands on a blue background representing areas of collagen digestion.

Isolation of RNA and Real-Time PCR

Total RNA was isolated from individual cells or tissues by using the RNeasy Mini Kit or RNeasy Micro Kit according to the manufacturer's instructions. cDNA was synthesized using 1 μg and the High-Capacity cDNA Reverse Transcription Kit (catalog 4368813; Thermo) according to the protocol specified by the manufacturer. Gene expression was measured using cDNA, SYBR, or TaqMan primers in real-time PCR. GAPDH was measured as a housekeeping gene. The relative amount of mRNA to GAPDH was calculated using the equation $2^{\Delta CT}$, in which $\Delta CT = CT_{gene} - CT_{GAPDH}$.

Verification of Twist1 Deletion in Peritoneal Macrophages from MKO

Peritoneal wash fluid was harvested from naive mice 4 days after an i.p. injection of 3% thioglycollate, as previously described,[17] and then suspended in FACS buffer for fluorescent cell sorting using FITC-labeled anti-F4/80, anti-Thy1.1, or anti-CD19 for macrophages, T cells, and B cells, respectively. The purity of the macrophage preparation was 99%. We then isolated RNA from these purified cells and detected Twist1 in macrophages, T cells, B cells, and other organs as shown in Figure 1.

Primary Peritoneal Macrophage Isolation and Activation Treatment

Primary mouse peritoneal macrophages were harvested from the peritoneal exudates of 6- to 8-week-old WT and MKO mice. The peritoneal exudate cells were washed twice with PBS solution, adjusted to 1×10^6 cells/ml in complete DMEM (Gibco) and cultured for 3–4 hours at 37°C and 5% carbon dioxide. Nonadherent cells were then removed by washing with warm PBS. Adherent cells were changed to serum-free medium and preconditioned with 150 IU/ml IFNγ (catalog 4031; Invitrogen) for 6 hours and then stimulated with 100 ng/ml LPS (catalog L2630; Sigma-Aldrich).

Monocyte Macrophage Isolation from Obstructed Kidneys

Kidneys were harvested and minced, followed by incubation with 0.1% collagenase type 1 (catalog 17100-017; Gibco) for 30 minutes at 37°C. Single cell suspensions were obtained by filtering through a 40-μm cell strainer. Thereafter, cells were stained with fluorescently labeled anti-CD45, anti-CD11b, anti-Ly6C, and anti-CX3CR1 (BD Bioscience), and subjected to fluorescent cell sorting. The gating strategy was as follows: first gate on single cells, second gate on $CD45^+$ cells, and third gate on $CD11b^+$ cells. Cells from MKO and WT meeting these criteria were then separated by Ly6C-high or -low staining and saved for real-time PCR. Similarly, cells expressing CD11b and CX3CR1 from WT and RKO mice were isolated and saved for real-time PCR.

Kidney Flow Cytometry

Flow cytometry of single cell suspensions from obstructed kidneys was performed as previously described.[21,22] Briefly, to achieve homogenization, obstructed kidneys underwent mechanical dissociation and enzymatic digestion. Cell suspensions were then filtered through 70- and 40-μm cell strainers. The resulting single cells were incubated with Fc Block for 20 minutes at 4°C and then stained with CD45, CD11b,

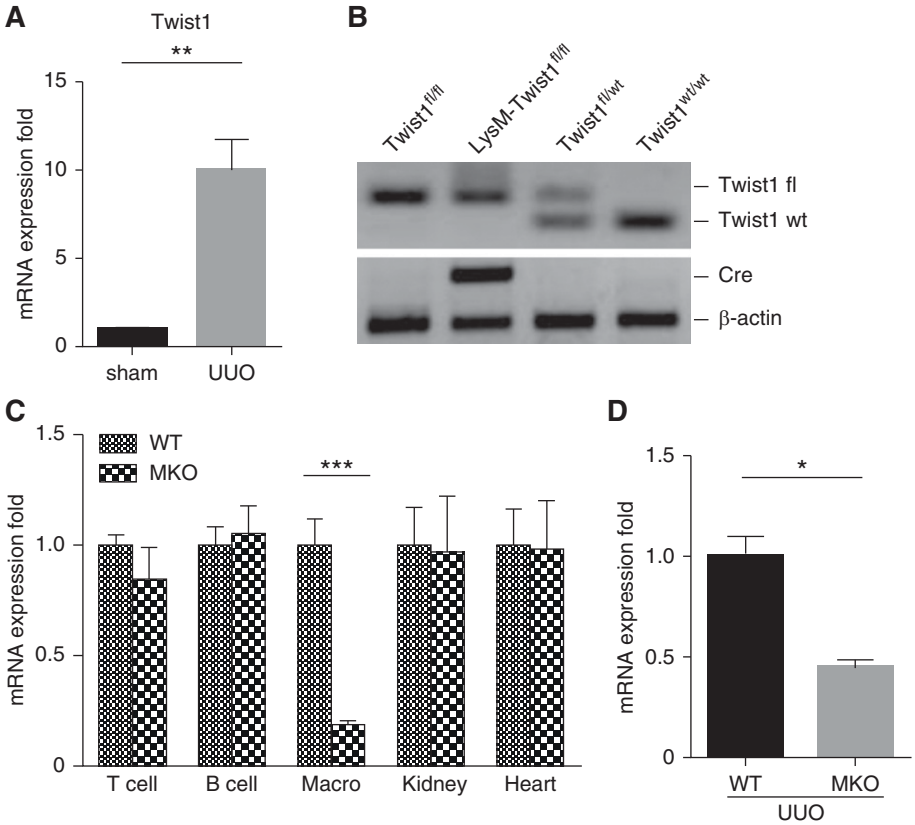

Figure 1. Verification of Twist1 deficiency in peritoneal macrophages and UUO kidneys from MKO mice. (A) Twist1 mRNA expression in kidneys from sham and UUO mice (n=3). (B) Genotyping the mice by PCR analysis of genomic DNA. (C) Verification of macrophage-specific deletion of Twist1 in MKO mice. mRNA expression for Twist1 in isolated peritoneal macrophages ("Macro"), T cells, B cells, and in whole kidney and heart from WT and MKO animals (n=6). (D) Twist1 mRNA expression in kidneys from WT and MKO mice after UUO ($n\geq7$). Data represent the mean±SEM. *$P<0.05$, **$P<0.01$, ***$P<0.001$. fl, floxed; UUO, unilateral ureteral obstruction; MKO, LysM-Cre; Twist1$^{fl/fl}$; WT, wild type.

Ly6G, Ly6C, CD4, and CD8 for 30 minutes at 4°C. Cells were washed and fixed with fixation/permeabilization buffer and analyzed on an LSRII flow cytometer (BD Biosciences).

Statistical Analyses

The values of each parameter within a group are expressed as the mean±SEM. For comparisons between groups with normally distributed data, statistical significance was assessed using the two-tailed unpaired t test. For comparisons between groups with non-normally distributed variables, we used the Wilcoxon test. Comparison among groups was performed with the one-way ANOVA test.

RESULTS

Twist1 Deletion in Infiltrating Macrophages Augments Collagen Deposition in the Obstructed Kidney

Twist1 in renal tubular cells plays an important role in EMT, but the actions of Twist1 in myeloid cells during renal fibrogenesis have not been established. To investigate the role of macrophage Twist1 in kidney fibrosis induced by UUO, we first confirmed the induction of Twist1 mRNA expression in whole kidney tissue after UUO. Indeed, mRNA expression of Twist1 was robust at 2 weeks after UUO compared with sham cohorts (1.0±0.06 versus 10.02±1.72 au; $P<0.01$) (Figure 1A). We have previously found prominent accumulation of LysM-expressing myeloid cells in the fibrotic kidney after UUO.[17] Thus, to isolate the functions Twist1 in these infiltrating myeloid cells, we crossed mice with a floxed allele for Twist1 with a line carrying Cre recombinase under the control of the LysM myeloid cell promotor (Figure 1B), thereby generating Twist1 "MKO" animals lacking Twist1 solely in LysM-expressing macrophages and Cre negative controls with normal Twist1 expression in kidney and heart (Figure 1C). We subjected WT and MKO mice to UUO, and at 14 days Twist1 mRNA expression in the fibrotic kidneys from MKO mice was markedly downregulated in comparison with WT mice (1.0±0.10 versus 0.45±0.04 au; $P<0.001$) (Figure 1D). Thus, Twist1 expression in activated, infiltrating macrophages accounts for half of all Twist1 expression in the obstructed kidney at day 14.

We then tested whether deleting Twist1 selectively within infiltrating myeloid cells influences the development of UUO-induced interstitial fibrosis. Twist1 MKO mice developed more severe kidney fibrosis 2 weeks after UUO compared with WTs as quantitated by hydroxyproline assay (10.7±0.8 versus 8.2±0.6 μg/10 mg; $P<0.05$; Figure 2A). Immunohistochemistry staining confirmed augmented collagen-I deposition in the interstitium of fibrotic kidneys from MKO mice compared with controls (Figure 2B), and Western blots showed significantly more collagen I, collagen IV, fibronectin, and α-SMA protein in the obstructed MKO kidneys versus WT controls (Figure 2, C and D). Enhanced accumulation of myofibroblasts in the obstructed MKO kidneys was confirmed by α-SMA staining (Supplemental Figure 1). Prior studies have demonstrated that Twist1 attenuates proinflammatory cytokine expression by suppressing NF-κB activation.[23] Among these mediators, C-C Motif Chemokine Ligand 2 (CCL2), TNF-α, IL-1β, and IFNγ have each been implicated in renal fibrogenesis, but their levels of mRNA expression were similar in the obstructed WT and MKO kidneys at day 14 (Figure 2E). Surprisingly, despite the exaggerated collagen deposition at the protein level and augmented myofibroblast accumulation in the MKO kidneys, mRNA levels for collagen I, fibronectin, and the fibrosis mediator TGFβ1 were similar in the groups (Figure 2F). Moreover, mRNA levels for the kidney injury marker Kim-1 were similar in the two groups (Supplemental Figure 2). These results suggest that Twist1 in inflammatory macrophages may regulate collagen degradation rather than tissue injury and collagen deposition during renal scar formation.

Twist1 in Myeloid Cells Promotes MMP13 Generation in the Fibrosing Kidney

MMPs are key drivers of collagen degradation, and Twist1 has been shown to regulate MMPs in nonrenal tissues, for example, MMP1 in melanoma cells and MMP3 in chondrocytes.[11,12] Moreover, some MMPs are released by macrophages to degrade ECM and ameliorate organ fibrosis.[24–28] We therefore broadly profiled the expression of the MMP family members in the obstructed kidney at day 14 (Figure 3A). Obstructed MKO kidneys showed significantly lower expression of MM9, MMP11, and MMP13 mRNA compared with obstructed WT controls. However, MMP9 can promote rather than ameliorate renal fibrosis. MMP11 is known to weakly degrade structural proteins of the ECM, but was not detectable in isolated macrophages from fibrotic kidneys or in peritoneal-derived macrophages *in vitro* (data not shown). By contrast, MMP13, also named collagenase 3, efficiently catalyzes collagen degradation and was gradually induced at the protein level over the 2 weeks after UUO (1.0±0.02, 1.4±0.14, 2.4±0.07 au, respectively; $P<0.01$) (Figure 3, B and D). Moreover, Twist1 deletion in LysM-expressing macrophages dramatically blunted MMP13 protein expression (1.0±0.05 versus 0.51±0.03 au; $P<0.001$) (Figure 3, C and E) in the obstructed kidney at 14 days. Collectively, our data indicate that Twist1 in inflammatory macrophages enhances MMP13 expression in fibrotic kidneys.

Twist1 Drives MMP13 Expression in CD11b$^+$Ly6C^{lo} Renal Myeloid Cells after UUO

We sought to determine whether MMP13 is regulated by Twist1 in infiltrating myeloid cells. To this end, we used fluorescent cell sorting to isolate CD11b$^+$ myeloid cells from obstructed WT and MKO kidneys (Figure 4, A and B). Sorted CD11b$^+$Ly6C^{hi} macrophages from the WT and MKO kidneys expressed similar mRNA levels for MMP13 (1.0±0.25 versus 1.1±0.10 au). MMP13 expression was markedly higher in CD11b$^+$Ly6C^{lo} macrophages from WT fibrotic kidneys than in their Ly6C^{hi} counterparts (1.0±0.25 versus 14.95±2.54 au; $P<0.001$). Compared with WT CD11b$^+$Ly6C^{lo} macrophages, CD11b$^+$Ly6C^{lo} macrophages from MKOs had dramatically lower levels of MMP13 mRNA expression (14.95±2.54 versus 4.26±0.50 au; $P<0.01$). Moreover, we confirmed robust deletion of Twist1 in Ly6C^{lo} myeloid cells from the MKO cohort (Figure 4C). Thus, these Ly6C^{lo} myeloid cells are a prominent source of Twist1-dependent MMP13 generation, and MMP13 expression in these cells is markedly attenuated by Twist1 deficiency. Importantly, the difference in renal MMP13 levels between groups is not driven by blunted Ly6C^{lo} myeloid cell infiltration because the numbers of these cells (Figure 4D) and also Ly6G$^+$ neutrophils, CD11b$^+$Ly6G$^-$ monocytes, and T lymphocytes (Supplemental Figure 3) were similar in the obstructed WT and MKO kidneys.

Next we investigated the effects of Twist1 on MMP13 generation in activated macrophages *in vitro*. Induction of MMP13 mRNA (Figure 5A) and protein (Figure 5, B and C) in activated peritoneal-derived macrophages was nearly abrogated by Twist1 deficiency. MMP13 activity was similarly attenuated in the supernatants from the activated MKO macrophages (Figure 5, B, bottom, and D).

Twist1 in CX3CR1-Resident Myeloid Cells Does Not Affect UUO-Induced Kidney Fibrosis or MMP13 Expression

CD11b$^+$Ly6C^{lo} macrophage subpopulations include those derived from converted Ly6C^{hi} macrophages after recruitment from the circulation but also tissue-resident, CX3CR1-expressing myeloid cells. To address the possibility that MMP13 secretion from these tissue-resident myeloid cells modulates renal fibrogenesis, we created transgenic mice with selective deficiency in CX3CR1-expressing cells (RKO mice) and subjected these animals and WT littermate controls to our UUO model. First, to validate the efficacy of the CX3CR1 Cre deleter, we observed that obstructed kidneys from CX3CR1 Cre$^+$ mT/mG reporter mice had robust Cre-mediated target gene recombination marked by green fluorescent protein fluorescence compared with obstructed Cre$^-$ controls (Figure 6A). We also confirmed robust deletion of Twist1 mRNA in CD11b$^+$CX3CR1$^+$ myeloid cells from RKO kidneys

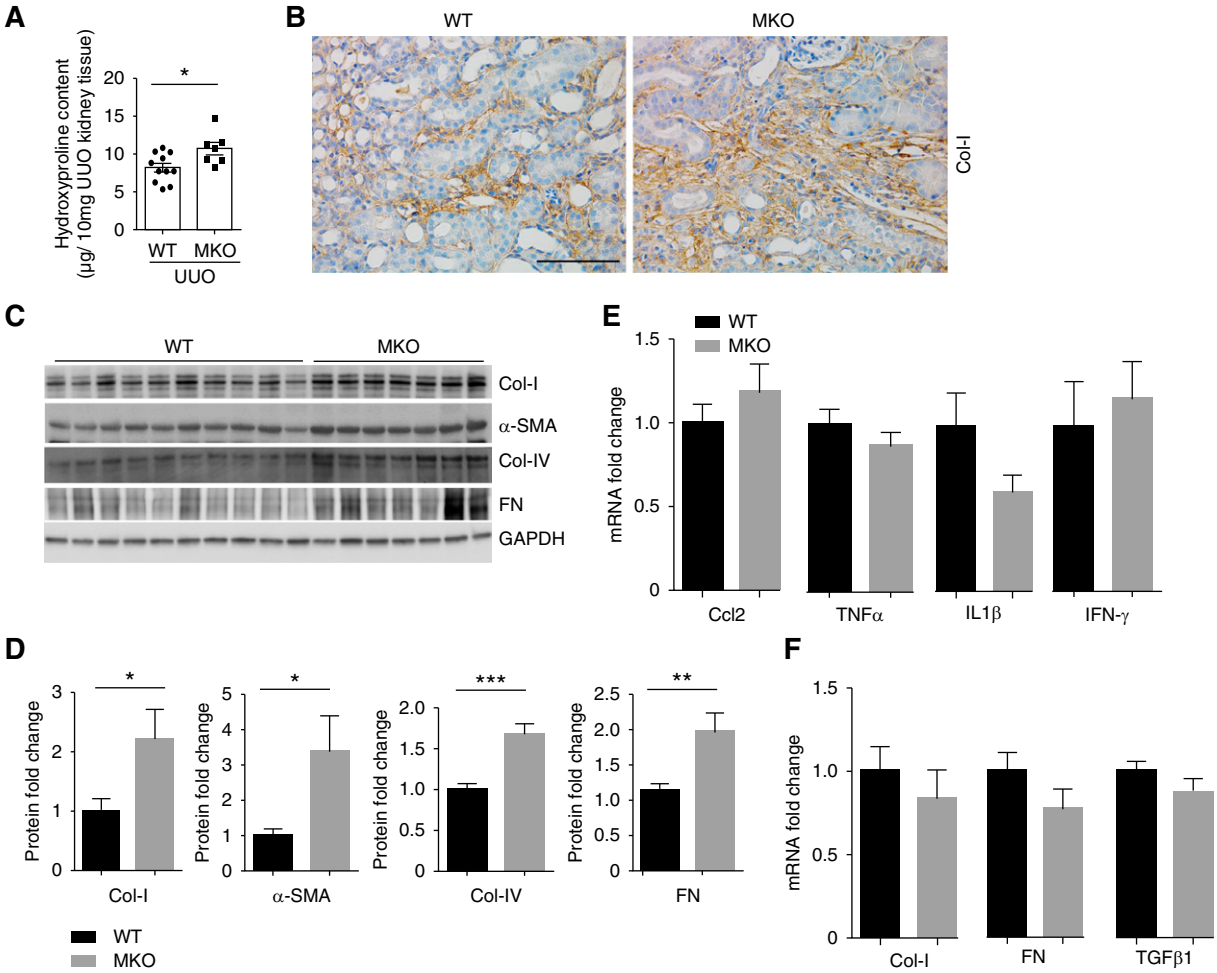

Figure 2. Twist1 deletion in macrophages augments collagen deposition in mice after ureteral obstruction. (A) Hydroxyproline content from obstructed WT and MKO kidneys after UUO at 2 weeks ($n \geq 7$). (B) Representative sections from obstructed WT and MKO kidneys stained with Col-I. Scale bar, 100 μm (C) Western blot for Col-I, α-SMA, Col-IV and FN in kidneys from WT and MKO mice after UUO at 2 weeks. (D) Semiquantitative determination of Col-I, α-SMA, Col-IV, and FN protein in the kidneys from WT and MKO mice after UUO ($n \geq 7$). (E) mRNA levels of inflammatory cytokines in obstructed kidneys from WT and MKO mice ($n \geq 7$). (F) mRNA levels of fibrosis markers/mediators in obstructed kidneys from WT and MKO mice ($n \geq 7$). Data represent the mean±SEM. *$P<0.05$, **$P<0.01$, ***$P<0.001$. Col-I, collagen-I; FN, fibronectin; α-SMA, α-smooth muscle actin; UUO, unilateral ureteral obstruction; MKO, LysM-Cre; Twist1$^{fl/fl}$; WT, wild type.

(Figure 6B). As shown in Figure 6, C and D, protein levels of type 1 collagen and α-SMA were similar in obstructed WT and RKO kidneys. Moreover, gene expressions for the panel of MMPs were also similar in obstructed kidneys of the two groups (Figure 6E). Thus, Twist1 in CX3CR1-resident myeloid cells is not required for MMP13 expression in obstructed kidneys and does not influence the severity of kidney fibrosis in our model.

MMP13 Inhibition Augments Renal Accumulation of Type 1 Collagen after UUO

Based on these data, we posited that Twist1 deletion in infiltrating LysM-expressing myeloid cells impairs MMP13-mediated ECM degradation, leading to exaggerated ECM accumulation after UUO in our Twist1 MKO cohort. To directly test this possibility, we treated WT and MKO animals after UUO with an MMP13 selective inhibitor CL82198 (10 mg/kg per day, i.p.).[18,19] MMP13 inhibition augmented levels of type 1 collagen and α-SMA protein after UUO only in the WT animals and abrogated the differences in these markers between the WT and MKO cohorts (Figure 7). Thus, Twist1 suppresses myeloid cell–dependent fibrosis in the kidney through effects on MMP13-dependent matrix degradation.

DISCUSSION

In this study, we demonstrate that deletion of Twist1 in LysM-expressing activated macrophages affects ECM degradation

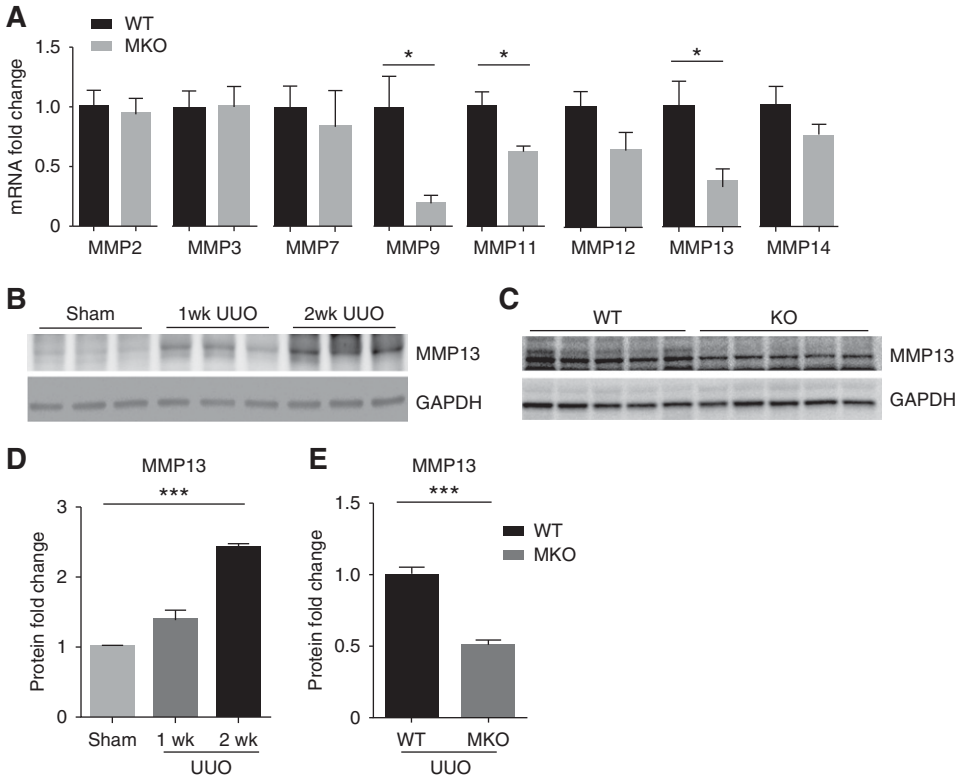

Figure 3. Twist1 in myeloid cells promotes MMP13 generation in the fibrosing kidney. (A) mRNA expressions for MMPs in the kidneys from WT and MKO mice with UUO after 2 weeks ($n \geq 7$). (B) Progressive induction of MMP13 in the scarred kidney after UUO. (C) MMP13 protein levels determined by Western blotting in obstructed kidneys from WT and MKO mice after UUO at 2 weeks. (D and E) Semiquantitative determination of MMP13 protein from blots in B ($n=3$) and C ($n \geq 7$), respectively. Data represent the mean±SEM. *$P<0.05$, ***$P<0.001$. GAPDH, glyceraldehyde-3-phosphate dehydrogenase; MMP, matrix metalloproteinase; MMP13, matrix metallopeptidase 13; UUO, unilateral ureteral obstruction; MKO, LysM-Cre; Twist1$^{fl/fl}$; WT, wild type.

rather than deposition in a murine model of aggressive renal fibrogenesis, confirming that enzyme-mediated matrix turnover and degradation play key roles in the renal ECM accumulation. MMP13 abundance in whole kidney and CD11b^{+}Ly6C^{lo} macrophages from MKO mice after UUO is significantly lower than in WT controls, and treatment with an MMP13 inhibitor in the UUO model equalizes renal scar formation in the MKO and WT cohorts. To our knowledge, these experiments are the first evidence that Twist1 in infiltrating myeloid cells significantly induces MMP13 in CD11b^{+}Ly6C^{lo} macrophages with consequent ECM degradation and attenuation of UUO-induced renal interstitial fibrosis.

Twist1 is a transcription factor that regulates cell migration, proliferation, immune function, mesoderm formation, and differentiation *via* the induction of several downstream targets. The MMP protein family is one of the most important targets of Twist1. For example, Twist1 binds to the MMP1 promoter, increasing MMP1 expression to drive migration and invasion of tumor cells *via* ERK1/2 signaling.[12] More broadly, transfection of Twist1 into human chondrocytes upregulates mRNA levels of MMP2, 3, 8, 9, 10, 11, 12, and 13.[11] MMP13 is also regulated by a T-box transcription factor, Tbx20, which is another target gene of Twist1, and gain- and loss-of-function experiments affecting Tbx20 and Twist1 levels provide clear evidence for an important role of Twist1 in regulating MMP13 expression in nonimmune cell lineages.[29,30] Nevertheless, Twist1 deletion did not affect levels of Tbx20-dependent inflammatory cytokines in the obstructed kidney. In our studies, Twist1 deletion in activated macrophages diminishes the expression of MMP9, 11, and 13 in the fibrotic kidney. MMP9 can promote EMT by degrading type 4 collagen and laminin and disrupting the integrity of the tubular cell membrane, which contributes to the development of fibrotic disorders.[31–33] Thus, reduced MMP9 expression in the obstructed Twist1 MKO kidneys cannot account for their exaggerated fibrosis. Although MMP11 can degrade ECM,[34] we were unable to detect MMP11 within myeloid cells infiltrating the fibrosing kidney. We therefore posited that blunted MMP13 expression may account for the augmented renal fibrosis seen with myeloid Twist1 deficiency.

MMP13, also known as collagenase 3, strongly cleaves collagen-I not only at a site in the triple helix but also in

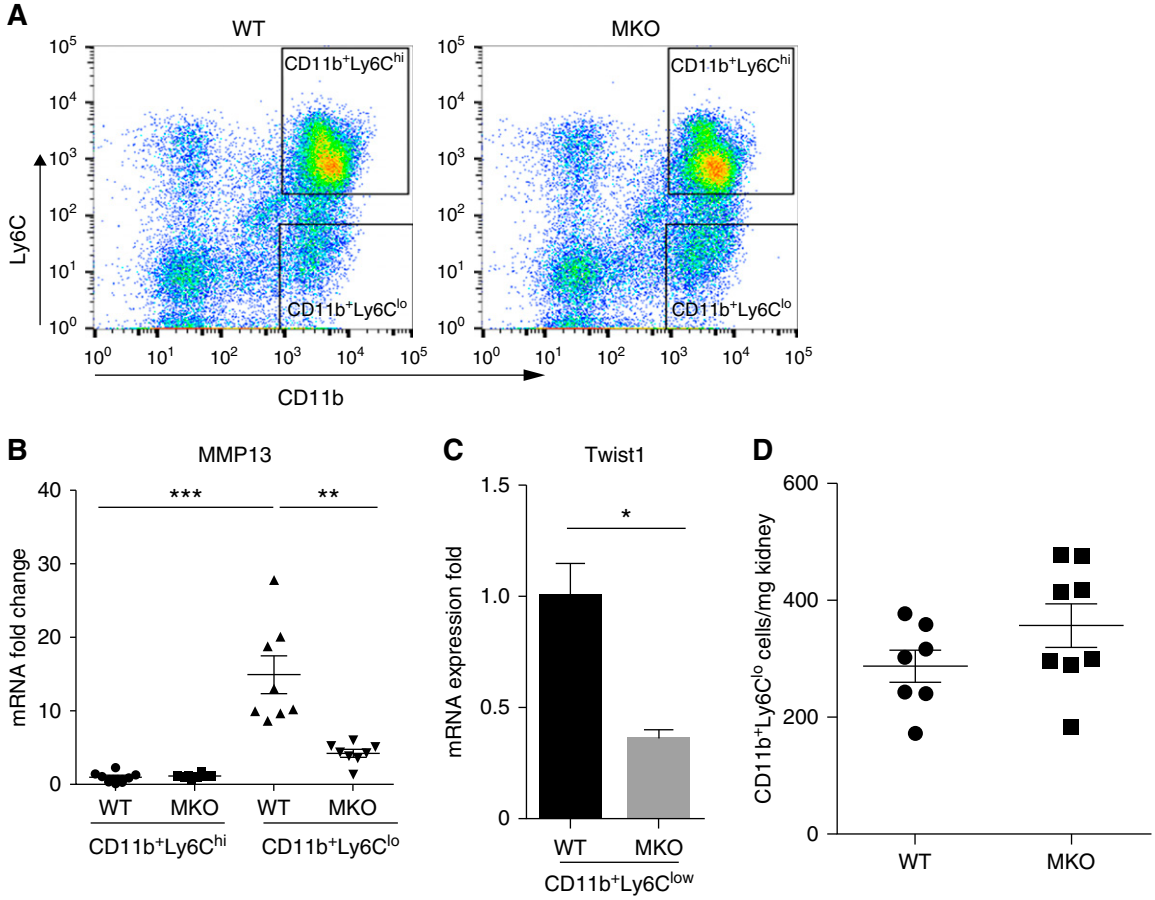

Figure 4. Twist1-dependent generation of MMP13 in CD11b$^+$Ly6C^{lo} renal myeloid cells constrains renal fibrogenesis. (A) Representative flow plots of CD11b versus Ly6C staining from obstructed kidneys of WT and MKO mice after UUO at 2 weeks. (B) mRNA level for MMP13 in CD11b$^+$ Ly6C^{hi} or CD11b$^+$ Ly6C^{lo} myeloid cells from obstructed kidney (n=8). (C) mRNA level for Twist1 in CD11b$^+$ Ly6C^{lo} myeloid cells from WT- and MKO-obstructed kidneys at 2 weeks (n=3). (D) The number of CD11b$^+$ Ly6C^{lo} myeloid cells from WT- and MKO-obstructed kidneys at 2 weeks (n=7–8). Data represent the mean±SEM. *P<0.05, **P<0.01, ***P<0.001. MMP13, matrix metallopeptidase 13; UUO, unilateral ureteral obstruction; MKO, LysM-Cre; Twist1$^{fl/fl}$; WT, wild type.

the amino-terminal telopeptide which destabilizes crosslinked collagen.[24,35] These processes facilitate the breakdown of mature, highly crosslinked collagen in tissues. In several nonrenal tissues, MMP13 is required for appropriate remodeling of ECM. For example, MMP13 drives collagen breakdown within atherosclerotic plaques,[36–38] and after CCL4-induced liver injury, MMP13-deficient mice develop persistent hepatic fibrosis due to loss of MMP13-directed matrix resolution.[24] Inversely, overexpression of MMP13 promotes hepatic recovery from experimental liver cirrhosis.[39] Finally, MMP13 can cleave and inactivate several chemokines including CCL2, CCL7, and CXCL12 which attract immune cells into injured sites to enhance inflammatory and fibrotic responses.[40–42] Thus, MMP13 acts through several mechanisms to attenuate scar formation.

Myeloid cells are a key source of MMP13. Macrophages can drive scar formation *via* the production of profibrotic cytokines or degrade matrix *via* the generation of MMPs. Because we did not detect differences between our experimental groups in renal levels of inflammatory cytokines, we focused on the capacity of myeloid cell Twist1 to limit fibrogenesis *via* effects on MMP13 elaboration. Renal expression of MMP13 increased steadily after UUO, peaking at 2 weeks, concomitant with maximum macrophage accumulation. Although we posited that Ly6C^{hi} inflammatory macrophages might produce MMP13, we detected far higher levels of MMP13 in the Ly6C^{lo} myeloid subset. This subset has been implicated in renal fibrogenesis after ischemia reperfusion.[4] Within this population, Twist1 deficiency blunted MMP13 induction by 70%. These myeloid cells may also correspond to the MMP13-producing "scar-associated macrophages" detected in the fibrotic liver, although markers are inconsistent across tissues.[24] In the liver, MMP13 mRNA expression is largely restricted to regions of fibrosis that are rich in scar-associated macrophages, and deleting these cells attenuates MMP13 expression. Our studies reveal that MMP13 produced by Ly6C^{lo} macrophages is similarly a critical inhibitor of scar formation in the injured kidney.

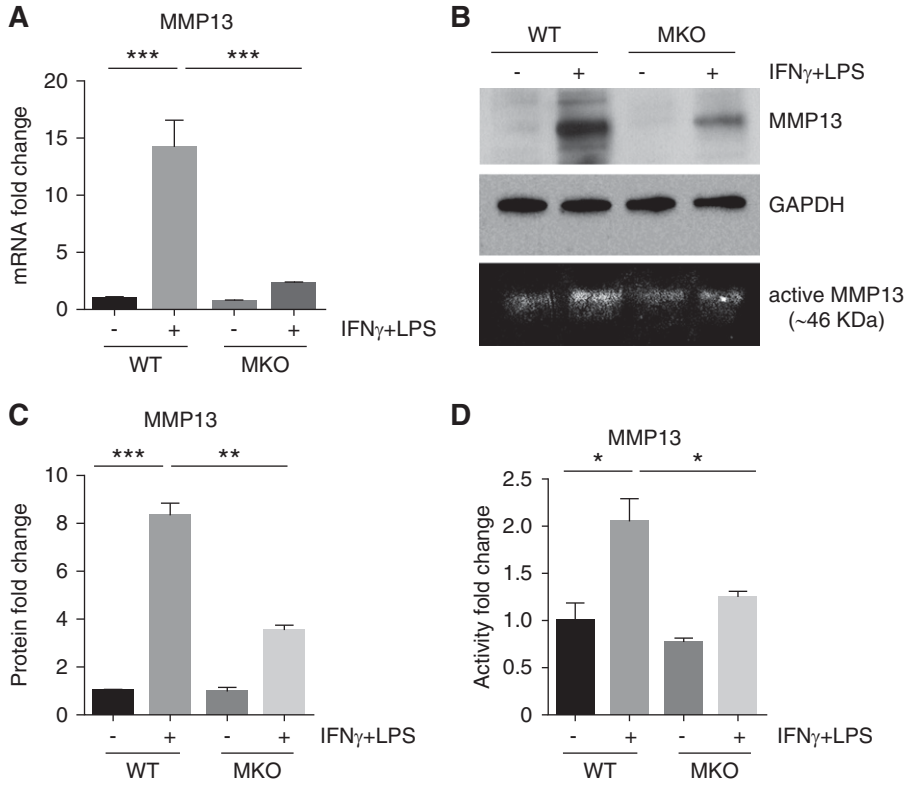

Figure 5. Twist1-deficient peritoneal macrophages (MKO) have blunted induction of MMP13 after *in vitro* activation by IFNγ plus LPS treatment. (A) mRNA levels of MMP13 in WT versus MKO macrophages from groups as indicated. (B) Western blots of MMP13 protein in WT versus MKO macrophages with collagen-zymographic analysis of MMP13 activity in macrophage culture supernatants shown on bottom. (C) Determination of MMP13 protein levels from B using densitometry (n=3). (D) Zymographic analysis of relative MMP13 activity levels in supernatants from WT versus MKO macrophage cultures (n=3). Data represent the mean±SEM. *P<0.05, **P<0.01, ***P<0.001. GAPDH, glyceraldehyde-3-phosphate dehydrogenase; MMP13, matrix metallopeptidase 13; MKO, LysM-Cre; Twist1$^{fl/fl}$; WT, wild type.

The two major subsets of murine monocytes that differentiate into macrophages are distinguished by two constellations of surface markers: CCR2^{+}CX3CR1^{lo}Ly6C^{hi} and CCR2^{-}CX3CR1^{hi}Ly6C^{lo}.[5] Under normal conditions, Ly6C^{lo} myeloid cells are located in the interstitium to surveil endothelial cells and surrounding tissues and replenish by self-proliferation.[43] However, in the setting of diseases, Ly6C^{lo} macrophages may be derived from self-proliferation of resident macrophages or conversion of Ly6C^{hi} macrophages recruited from the circulation. To identify the primary source of the Ly6C^{lo} macrophage subpopulation during renal fibrogenesis, we generated mice with Twist1 deficiency in resident macrophages. However, we found that deletion of Twist1 in CX3CR1-expressing myeloid cells did not influence MMP13 generation and/or progression of kidney fibrosis, suggesting that the Ly6C^{lo} macrophages producing MMP13 in the obstructed kidney are derived from the circulation. These studies also suggest that MMP13 produced by CX3CR1^{+} renal dendritic cells is not critical to the maintenance of renal architecture.[44] Our findings are also consistent with those of Ramachandran *et al.*[25] who found that, in the healing liver, Ly6C^{lo} rather than Ly6C^{hi} macrophages represent the principal subset expressing MMPs, including MMP2, 9, 12, and 13. According to previous studies, M1 macrophages express high levels of pro-inflammatory cytokines, whereas M2 macrophages elaborate high levels of anti-inflammatory cytokines. As in our studies, these MMP13-producing cells do not fit neatly into the M1/M2 paradigm of macrophage polarization.[26]

We acknowledge that our study has some limitations. We recognize that the genetic targeting tools we have applied are not completely specific. For example, LysM can be expressed on neutrophils,[45] but these tools represent the use of the best available technology for our purposes. Second, the UUO model induces vigorous inflammation in the kidney. For this reason, the model is appropriate for investigating macrophage functions. Nevertheless, in future studies, interactions between Twist1 and MMP13 will need to be investigated in other models of tissue fibrosis.

In sum, our experiments indicate that Twist1 produced by recruited myeloid cells direct degradation of ECM in the injured kidney *via* the upregulation of MMP13. The upregulation of Twist1 and MMP13 in human CKD suggests that

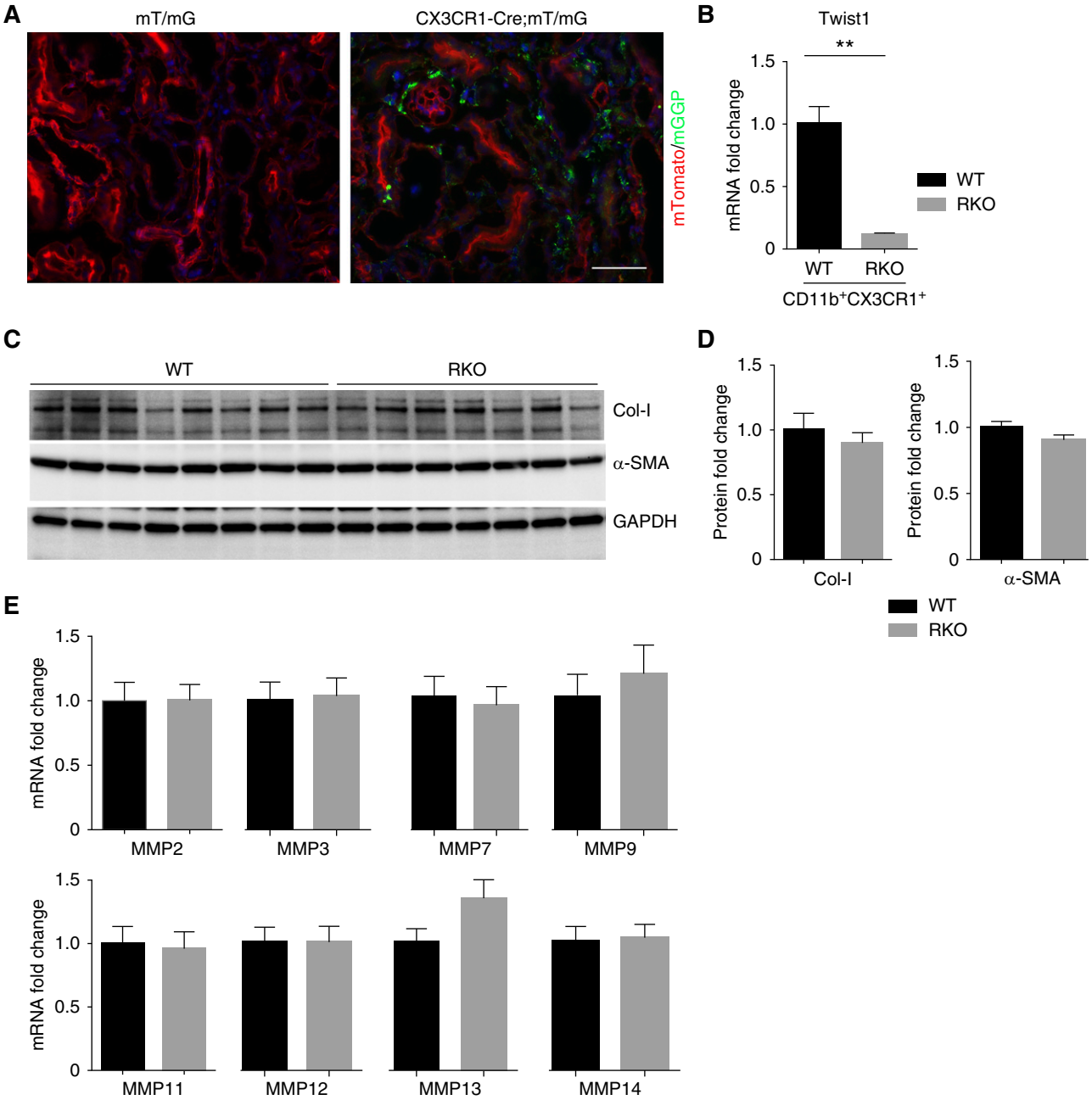

Figure 6. Twist1 in CX3CR1-expressing myeloid cells does not affect UUO-induced kidney fibrosis or MMP13 expression. (A) Representative sections of obstructed kidneys from mT/mG and CX3CR1 Cre^{+} mT/mG reporter mice in which CX3CR1-expressing resident myeloid cells fluoresce green and all other tissues fluoresce red. Scale bar, 100 μm. (B) mRNA levels for Twist1 in CD11b^{+}CX3CR1^{+} myeloid cells isolated from WT- and RKO-obstructed kidneys (n=3). (C) Western blot for Col-I and α-SMA in kidneys from WT and RKO mice after UUO at 2 weeks. (D) Semiquantitative determination of Col-I and α-SMA in the kidneys from WT and RKO mice after UUO ($n\geq7$). (E) mRNA expressions for MMPs in the kidneys from WT and RKO mice with UUO after 2 weeks ($n\geq7$). Data represent the mean±SEM. **$P<0.01$. Col-I, collagen I; MMP, matrix metalloproteinase; MMP13, matrix metallopeptidase 13; α-SMA, α-smooth muscle actin; UUO, unilateral ureteral obstruction; RKO, CX3CR1-Cre; Twist1$^{fl/fl}$; WT, wild type.

our findings have relevance to human disease.[46,47] The protective actions of Twist1 in myeloid cells are surprising given the known profibrotic actions of Twist1 in intrinsic renal parenchymal cells.[8] These studies demonstrate the need for a broad understanding of the cell-specific actions of mediators involved in kidney fibrogenesis to guide the design of pharmacologic interventions with minimal off-target side effects.

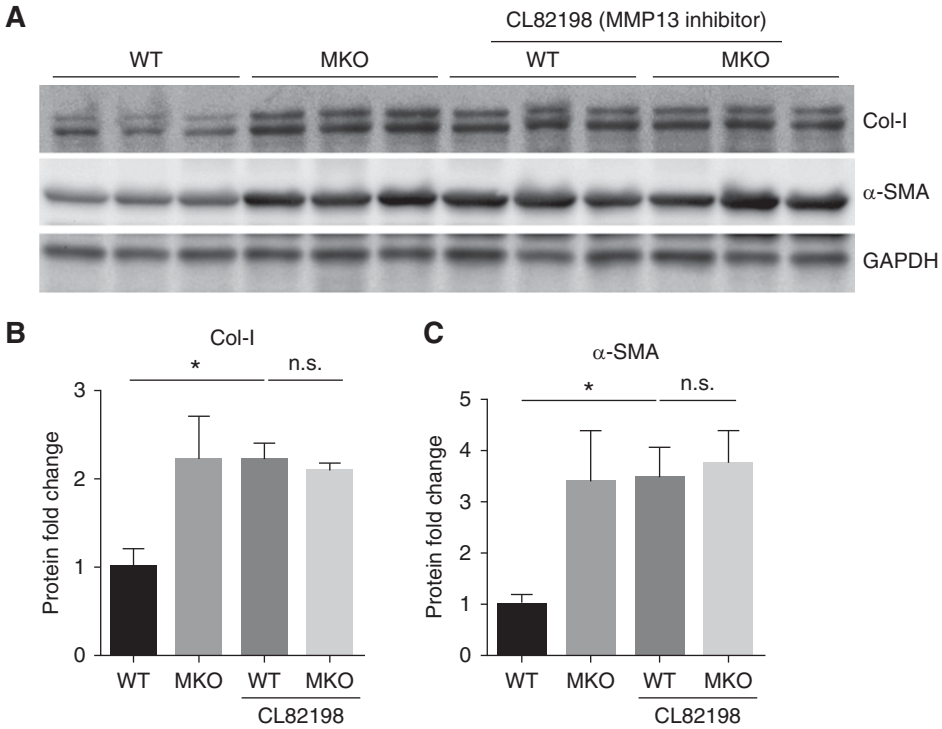

Figure 7. MMP13 inhibition augments levels of type 1 collagen and α-SMA protein after UUO. (A) Western blot for Col-I and α-SMA protein in obstructed kidneys from WT and MKO mice who were treated with vehicle or CL82198 (MMP13 inhibitor, intraperitoneally) daily for 2 weeks after UUO. (B and C) Semiquantitative determination of Col-I and α-SMA from C ($n \geq 7$). Data represent the mean±SEM. *$P<0.05$. Col-I, collagen 1; GADPH, glyceraldehyde-3-phosphate dehydrogenase; MMP13, matrix metallopeptidase 13; n.s., not significant; α-SMA, α-smooth muscle actin; UUO, unilateral ureteral obstruction; MKO, LysM-Cre; Twist1$^{fl/fl}$; WT, wild type.

ACKNOWLEDGMENTS

Dr. Ren and Dr. Crowley designed the study. Dr. Ren, Dr. Zhang, Dr. Rudemiller, Mr. Griffiths, Dr. Wen, and Dr. Lu conducted the experiments. Dr. Ren, Dr. Privratsky, and Dr. Crowley analyzed the data. Dr. Ren and Dr. Crowley drafted the manuscript. Dr. Crowley revised and edited the manuscript. Dr. Gunn kindly provided the CX3CR1 Cre mouse line.

DISCLOSURES

None.

FUNDING

The authors acknowledge funding from the NIH grants DK087893 and HL128355; grant BX000893; and American Heart Association award 18TPA34170047.

SUPPLEMENTAL MATERIAL

This article contains the following supplemental material online at http://jasn.asnjournals.org/lookup/suppl/doi:10.1681/ASN.2018121253/-/DCSupplemental.

Supplemental Figure 1. Enhanced myofibroblast accumulation in obstructed MKO kidneys.

Supplemental Figure 2. mRNA levels of Kim-1 in obstructed WT and MKO kidneys.

Supplemental Figure 3. Immune cell infiltration into WT and MKO kidneys following UUO.

Supplemental Figure 4. The gating strategy for sorting viable CD11b+CX3CR1+ myeloid cells from WT and RKO kidneys.

REFERENCES

1. Duffield JS: Cellular and molecular mechanisms in kidney fibrosis. *J Clin Invest* 124: 2299–2306, 2014
2. Eddy AA: Overview of the cellular and molecular basis of kidney fibrosis. *Kidney Int Suppl (2011)* 4: 2–8, 2014
3. Liu Y: Cellular and molecular mechanisms of renal fibrosis. *Nat Rev Nephrol* 7: 684–696, 2011
4. Clements M, Gershenovich M, Chaber C, Campos-Rivera J, Du P, Zhang M, et al.: Differential Ly6C expression after renal ischemia-reperfusion identifies unique macrophage populations. *J Am Soc Nephrol* 27: 159–170, 2016
5. Dick SA, Macklin JA, Nejat S, Momen A, Clemente-Casares X, Althagafi MG, et al.: Self-renewing resident cardiac macrophages limit adverse remodeling following myocardial infarction. *Nat Immunol* 20: 29–39, 2019
6. Meng XM, Tang PM, Li J, Lan HY: Macrophage phenotype in kidney injury and repair. *Kidney Dis (Basel)* 1: 138–146, 2015

7. Ricardo SD, van Goor H, Eddy AA: Macrophage diversity in renal injury and repair. *J Clin Invest* 118: 3522–3530, 2008
8. Lovisa S, LeBleu VS, Tampe B, Sugimoto H, Vadnagara K, Carstens JL, et al.: Epithelial-to-mesenchymal transition induces cell cycle arrest and parenchymal damage in renal fibrosis. *Nat Med* 21: 998–1009, 2015
9. Lin SL, Kisseleva T, Brenner DA, Duffield JS: Pericytes and perivascular fibroblasts are the primary source of collagen-producing cells in obstructive fibrosis of the kidney. *Am J Pathol* 173: 1617–1627, 2008
10. Humphreys BD, Lin SL, Kobayashi A, Hudson TE, Nowlin BT, Bonventre JV, et al.: Fate tracing reveals the pericyte and not epithelial origin of myofibroblasts in kidney fibrosis. *Am J Pathol* 176: 85–97, 2010
11. Hasei J, Teramura T, Takehara T, Onodera Y, Horii T, Olmer M, et al.: TWIST1 induces MMP3 expression through up-regulating DNA hydroxymethylation and promotes catabolic responses in human chondrocytes. *Sci Rep* 7: 42990, 2017
12. Weiss MB, Abel EV, Mayberry MM, Basile KJ, Berger AC, Aplin AE: TWIST1 is an ERK1/2 effector that promotes invasion and regulates MMP-1 expression in human melanoma cells. *Cancer Res* 72: 6382–6392, 2012
13. Niesner U, Albrecht I, Janke M, Doebis C, Loddenkemper C, Lexberg MH, et al.: Autoregulation of Th1-mediated inflammation by twist1. *J Exp Med* 205: 1889–1901, 2008
14. Pham D, Walline CC, Hollister K, Dent AL, Blum JS, Firulli AB, et al.: The transcription factor Twist1 limits T helper 17 and T follicular helper cell development by repressing the gene encoding the interleukin-6 receptor α chain. *J Biol Chem* 288: 27423–27433, 2013
15. Sharif MN, Sosic D, Rothlin CV, Kelly E, Lemke G, Olson EN, et al.: Twist mediates suppression of inflammation by type I IFNs and Axl. *J Exp Med* 203: 1891–1901, 2006
16. Chen YT, Akinwunmi PO, Deng JM, Tam OH, Behringer RR: Generation of a Twist1 conditional null allele in the mouse. *Genesis* 45: 588–592, 2007
17. Zhang JD, Patel MB, Griffiths R, Dolber PC, Ruiz P, Sparks MA, et al.: Type 1 angiotensin receptors on macrophages ameliorate IL-1 receptor-mediated kidney fibrosis. *J Clin Invest* 124: 2198–2203, 2014
18. Wang M, Sampson ER, Jin H, Li J, Ke QH, Im HJ, et al.: MMP13 is a critical target gene during the progression of osteoarthritis. *Arthritis Res Ther* 15: R5, 2013
19. Waldron AL, Schroder PA, Bourgon KL, Bolduc JK, Miller JL, Pellegrini AD, et al.: Oxidative stress-dependent MMP-13 activity underlies glucose neurotoxicity. *J Diabetes Complications* 32: 249–257, 2018
20. Hu X, Beeton C: Detection of functional matrix metalloproteinases by zymography. *J Vis Exp* (45): 2445, 2010
21. Rudemiller NP, Patel MB, Zhang JD, Jeffs AD, Karlovich NS, Griffiths R, et al.: C-C motif chemokine 5 attenuates angiotensin II-dependent kidney injury by limiting renal macrophage infiltration. *Am J Pathol* 186: 2846–2856, 2016
22. Privratsky JR, Zhang J, Lu X, Rudemiller N, Wei Q, Yu YR, et al.: Interleukin 1 receptor (IL-1R1) activation exacerbates toxin-induced acute kidney injury. *Am J Physiol Renal Physiol* 315: F682–F691, 2018
23. Šošić D, Richardson JA, Yu K, Ornitz DM, Olson EN: Twist regulates cytokine gene expression through a negative feedback loop that represses NF-kappaB activity. *Cell* 112: 169–180, 2003
24. Fallowfield JA, Mizuno M, Kendall TJ, Constandinou CM, Benyon RC, Duffield JS, et al.: Scar-associated macrophages are a major source of hepatic matrix metalloproteinase-13 and facilitate the resolution of murine hepatic fibrosis. *J Immunol* 178: 5288–5295, 2007
25. Ramachandran P, Pellicoro A, Vernon MA, Boulter L, Aucott RL, Ali A, et al.: Differential Ly-6C expression identifies the recruited macrophage phenotype, which orchestrates the regression of murine liver fibrosis. *Proc Natl Acad Sci U S A* 109: E3186–E3195, 2012
26. Ma PF, Gao CC, Yi J, Zhao JL, Liang SQ, Zhao Y, et al.: Cytotherapy with M1-polarized macrophages ameliorates liver fibrosis by modulating immune microenvironment in mice. *J Hepatol* 67: 770–779, 2017
27. Wynn TA, Barron L: Macrophages: Master regulators of inflammation and fibrosis. *Semin Liver Dis* 30: 245–257, 2010
28. Anders HJ, Ryu M: Renal microenvironments and macrophage phenotypes determine progression or resolution of renal inflammation and fibrosis. *Kidney Int* 80: 915–925, 2011
29. Shelton EL, Yutzey KE: Tbx20 regulation of endocardial cushion cell proliferation and extracellular matrix gene expression. *Dev Biol* 302: 376–388, 2007
30. Shelton EL, Yutzey KE: Twist1 function in endocardial cushion cell proliferation, migration, and differentiation during heart valve development. *Dev Biol* 317: 282–295, 2008
31. Tan TK, Zheng G, Hsu TT, Wang Y, Lee VW, Tian X, et al.: Macrophage matrix metalloproteinase-9 mediates epithelial-mesenchymal transition *in vitro* in murine renal tubular cells. *Am J Pathol* 176: 1256–1270, 2010
32. Yang J, Shultz RW, Mars WM, Wegner RE, Li Y, Dai C, et al.: Disruption of tissue-type plasminogen activator gene in mice reduces renal interstitial fibrosis in obstructive nephropathy. *J Clin Invest* 110: 1525–1538, 2002
33. Wang X, Zhou Y, Tan R, Xiong M, He W, Fang L, et al.: Mice lacking the matrix metalloproteinase-9 gene reduce renal interstitial fibrosis in obstructive nephropathy. *Am J Physiol Renal Physiol* 299: F973–F982, 2010
34. Jones CB, Sane DC, Herrington DM: Matrix metalloproteinases: A review of their structure and role in acute coronary syndrome. *Cardiovasc Res* 59: 812–823, 2003
35. Ravanti L, Heino J, López-Otín C, Kähäri VM: Induction of collagenase-3 (MMP-13) expression in human skin fibroblasts by three-dimensional collagen is mediated by p38 mitogen-activated protein kinase. *J Biol Chem* 274: 2446–2455, 1999
36. Inada M, Wang Y, Byrne MH, Rahman MU, Miyaura C, López-Otín C, et al.: Critical roles for collagenase-3 (Mmp13) in development of growth plate cartilage and in endochondral ossification. *Proc Natl Acad Sci U S A* 101: 17192–17197, 2004
37. Stickens D, Behonick DJ, Ortega N, Heyer B, Hartenstein B, Yu Y, et al.: Altered endochondral bone development in matrix metalloproteinase 13-deficient mice. *Development* 131: 5883–5895, 2004
38. Deguchi JO, Aikawa E, Libby P, Vachon JR, Inada M, Krane SM, et al.: Matrix metalloproteinase-13/collagenase-3 deletion promotes collagen accumulation and organization in mouse atherosclerotic plaques. *Circulation* 112: 2708–2715, 2005
39. Endo H, Niioka M, Sugioka Y, Itoh J, Kameyama K, Okazaki I, et al.: Matrix metalloproteinase-13 promotes recovery from experimental liver cirrhosis in rats. *Pathobiology* 78: 239–252, 2011
40. Sen AI, Shiomi T, Okada Y, D'Armiento JM: Deficiency of matrix metalloproteinase-13 increases inflammation after acute lung injury. *Exp Lung Res* 36: 615–624, 2010
41. McQuibban GA, Butler GS, Gong JH, Bendall L, Power C, Clark-Lewis I, et al.: Matrix metalloproteinase activity inactivates the CXC chemokine stromal cell-derived factor-1. *J Biol Chem* 276: 43503–43508, 2001
42. McQuibban GA, Gong JH, Wong JP, Wallace JL, Clark-Lewis I, Overall CM: Matrix metalloproteinase processing of monocyte chemoattractant proteins generates CC chemokine receptor antagonists with anti-inflammatory properties *in vivo*. *Blood* 100: 1160–1167, 2002
43. Jenkins SJ, Ruckerl D, Cook PC, Jones LH, Finkelman FD, van Rooijen N, et al.: Local macrophage proliferation, rather than recruitment from the blood, is a signature of TH2 inflammation. *Science* 332: 1284–1288, 2011
44. Hochheiser K, Heuser C, Krause TA, Teteris S, Ilias A, Weisheit C, et al.: Exclusive CX3CR1 dependence of kidney DCs impacts glomerulonephritis progression. *J Clin Invest* 123: 4242–4254, 2013
45. Clausen BE, Burkhardt C, Reith W, Renkawitz R, Förster I: Conditional gene targeting in macrophages and granulocytes using LysMcre mice. *Transgenic Res* 8: 265–277, 1999
46. Sun S, Du R, Xia L, Sun W, Zhai Y, Yu Y, et al.: Twist is a new prognostic marker for renal survival in patients with chronic kidney disease. *Am J Nephrol* 35: 141–151, 2012
47. Henger A, Kretzler M, Doran P, Bonrouhi M, Schmid H, Kiss E, et al.: Gene expression fingerprints in human tubulointerstitial inflammation and fibrosis as prognostic markers of disease progression. *Kidney Int* 65: 904–917, 2004